Off-state leakage current reduction in AlGaN/GaN high electron mobility transistors by combining surface treatment and post-gate annealing

Off-state leakage current reduction in AlGaN/GaN high electron mobility transistors by combining surface treatment and post-gate annealing

Xing Lu[1], **Huaxing Jiang**[2], **Chao Liu**[2], **Xinbo Zou**[2] and **Kei May Lau**[2]

[1] State Key Laboratory of Electrical Insulation and Power Equipment, School of Electrical Engineering, Xi'an Jiaotong University, Xi'an, 710049, People's Republic of China
[2] Department of Electronic and Computer Engineering, Hong Kong University of Science and Technology, Clear Water Bay, Kowloon, Hong Kong

E-mail: eexlu@connect.ust.hk

CrossMark

Abstract

We report on the reduction of off-state leakage current in AlGaN/GaN high electron mobility transistors (HEMTs) by a two-step process combining pre-gate surface treatment and post-gate annealing (PGA), which suppressed the two leakage paths, namely, lateral surface leakage and vertical tunneling leakage, separately. The lateral surface leakage current, which was mainly induced by the high-density trap states generated during the device isolation etching process, was significantly reduced by a low power O_2-plasma and HCl surface treatment process. The PGA process reduced the vertical tunneling leakage current by improving the Schottky contact quality of the transistor gate. Consequently, the device off-state leakage current was decreased by about 7 orders of magnitude and no degradation was introduced to the on-state performance, leading to a high on/off current ratio of 10^{10} and steep subthreshold slope (SS) of 62 mV/dec. The origin and leakage suppression mechanisms are also investigated and discussed in detail.

Keywords: AlGaN/GaN, HEMT, post-gate annealing, off-state leakage current, surface treatment

(Some figures may appear in colour only in the online journal)

1. Introduction

Superior electrical and thermal properties have made AlGaN/GaN high electron mobility transistors (HEMTs) an attractive candidate for power switching and RF applications. However, high off-state leakage current remains a common issue affecting the device performance and reliability. In a typical HEMT structure, the off-state leakage current is comprised of vertical tunneling leakage and lateral surface leakage [1–3]. Figure 1 schematically shows the leakage paths for an AlGaN/GaN HEMT. In addition to the vertical tunneling gate leakage current ($I_{barrier}$) through the reverse biased Schottky barrier diode, a lateral leakage current ($I_{surface}$) assisted by the two-dimensional variable-range hopping of electrons through the high-density surface trap states occurs. The high-density trap states are normally induced by the residues, contaminations and defects formed during device fabrication, primarily, the dry etching process for mesa isolation. Previous studies have reported that the dry etching process in GaN-based devices produced deep level traps, causing significantly increased leakage current [4, 5]. Therefore, in some cases the off-sate leakage current for an AlGaN/GaN HEMT could be dominated by the trap-induced surface leakage through the probing pads, since the pads are normally located on the exposed GaN buffer by dry etching. In order to reduce the off-state leakage current, suppression of both vertical and lateral leakage paths are desirable. Various methods, including chemical or plasma treatment [6–10], thermal annealing
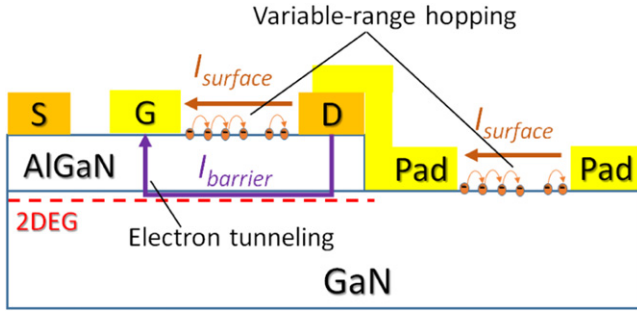
Figure 1. Leakage path model for an AlGaN/GaN HEMT: lateral surface leakage and vertical tunneling leakage.
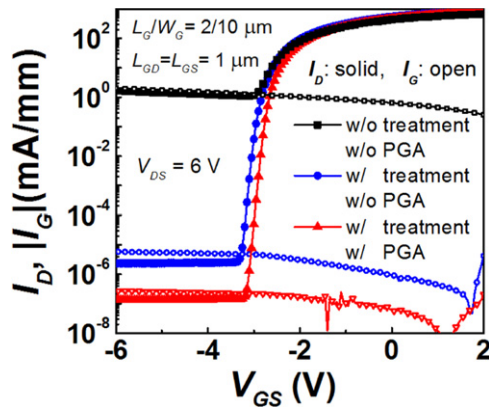
Figure 2. Transfer characteristics of the fabricated HEMTs on the three samples with 2 μm gate length (L_G) and 1 μm gate-to-source/gate-to-drain distances (L_{GS}/L_{GD}).
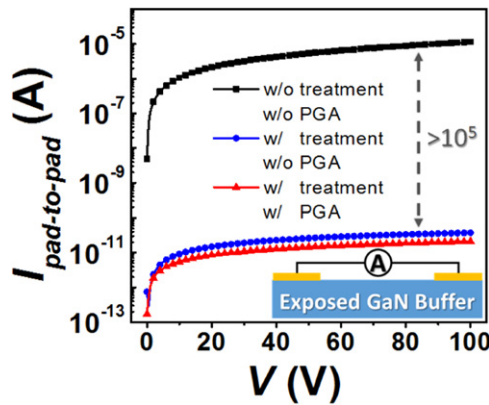
Figure 3. Comparison of leakage currents between two individual pads among the three samples. The pads are located on the exposed GaN buffer by dry etching and the inset shows the measured structure.

[11, 12], an oxide-filled isolation technique [12] and adding a p-InGaN cap layer [13], have been reported in the literature with a large reduction in the off-state leakage current for GaN-based HEMTs. However, such approaches usually introduce adverse effects to the device performance, for example, the decrease of channel conductivity. The origin and leakage suppression mechanisms in some of those approaches are still unclear.

In this study, we have developed a two-step process involving a pre-gate surface treatment and a post-gate annealing (PGA) to tackle the lateral surface leakage current and vertical tunneling leakage current separately. With the proposed surface treatment, the etch-induced trap states were effectively alleviated, leading to a significantly reduced pad-to-pad leakage current. The PGA process suppressed the vertical gate leakage current by improving the Schottky contact quality. Overall, the combined two-step process successfully reduced the off-state leakage current in AlGaN/GaN HEMTs by about 7 orders of magnitude without degrading the device on-state drain current. A high on/off current ratio of 10^{10} and a steep subthreshold swing (SS) of 62 mV/dec were achieved. Additionally, the three terminal off-state breakdown performance of the HEMTs was significantly improved.

2. Experiments

The AlGaN/GaN heterostructure used in this work was grown on a 2-inch sapphire substrate in an Aixtron 2400HT metal-organic chemical vapor deposition (MOCVD) system. The epilayer, from bottom to top, consists of a 300 nm AlN buffer layer, a 2.7 μm undoped GaN layer, a 1 nm AlN spacer, a 20 nm $Al_{0.25}Ga_{0.75}N$ barrier layer and, finally, a 2.5 nm undoped GaN cap layer. Room temperature Hall measurements showed a two-dimensional electron gas (2DEG) density of 9×10^{12} cm^{-2} and mobility of 1900 cm^2 V^{-1} s^{-1}. The fabrication of HEMTs started with mesa isolation using a BCl_3/Cl_2-based inductively coupled plasma (ICP) etching. Ti/Al/Ni/Au (20/150/50/80 nm) was deposited by e-beam evaporation and annealed at 850 °C for 30 s in a N_2 ambient to form the source/drain (S/D) Ohmic contact. Then, three cycles of O_2-plasma and HCl surface treatment were performed. One cycle surface treatment includes a one minute O_2-plasma with a low RF power of 100 W followed by a 20% HCl immersion for two minutes. After that, Ni/Au (20/200 nm) Schottky gate and probing pads were deposited simultaneously. Finally, a 30 min PGA at 300 °C in a N_2 ambient was performed. To make comparisons, two control samples were also prepared: one without surface treatment nor PGA, while the other went through surface treatment only but without PGA. After device characterization, SiN_x passivation using plasma enhanced chemical vapor deposition (PECVD) for the two fabricated HEMTs with and without the two-step surface treatment and PGA process was performed and further studied.

3. Results and discussion

Transfer characteristics of the fabricated HEMTs with 2 μm gate length (L_G) and 1 μm gate-to-source/gate-to-drain distances (L_{GS}/L_{GD}) on the three samples were performed and compared in figure 2. It clearly shows reduced off-state leakage currents with the pre-gate surface treatment and PGA. After a 3-cycle surface treatment, the off-state leakage current
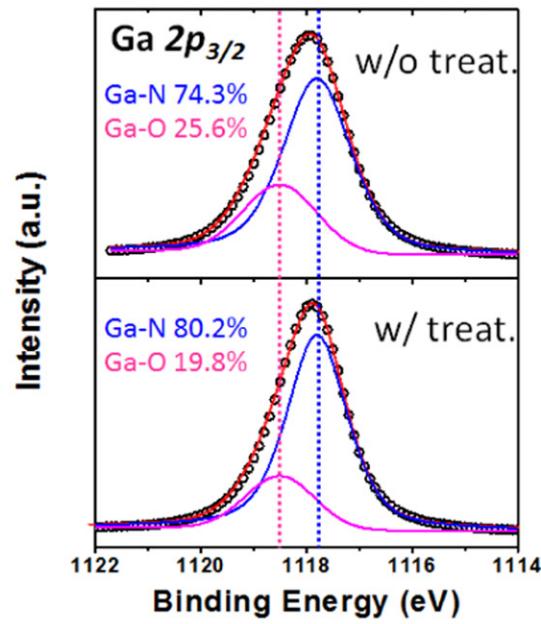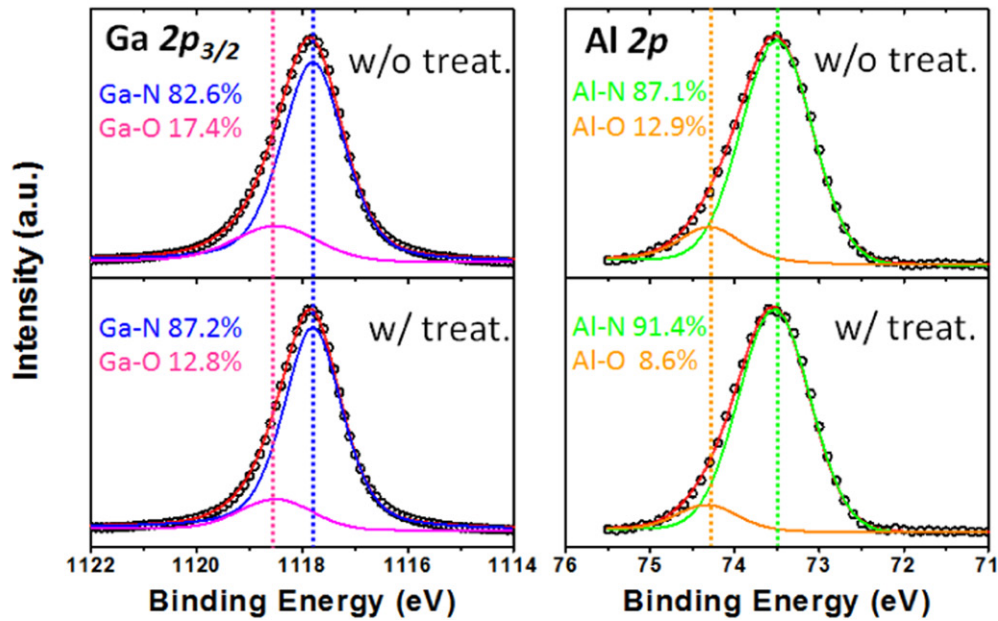
Figure 4. Ga $2p_{2/3}$ and Al $2p$ core-level spectra at the surfaces of both (a) the exposed GaN buffer and (b) the AlGaN barrier with and without surface treatment.

was reduced by over 5 orders of magnitude. The PGA further lowered the off-state leakage current by about 2 orders of magnitude. Consequently, a high on/off current ratio of 10^{10} and a sharp SS of 62 mV/dec were achieved for the device with both pre-gate surface treatment and PGA.

To investigate how the lateral surface leakage current was affected by the proposed two-step process, the *I-V* characterizations were performed between two individual Ni/Au pads located on exposed GaN buffer for the three samples,

as shown in figure 3. The inset of figure 3 illustrates the measured structure. The pad size is 100 μm by 100 μm, similar to the probing pads of the HEMT devices, and the pad-to-pad space is 100 μm. The leakage current between the individual pads for the sample without surface treatment nor PGA was as high as 10^{-5} A at 100 V, which is on the same order as the measured off-state leakage current of the HEMT on the same sample ($\sim$1 mA mm^{-1} for the 10 μm wide device, black curve in figure 2). It suggests that the high off-
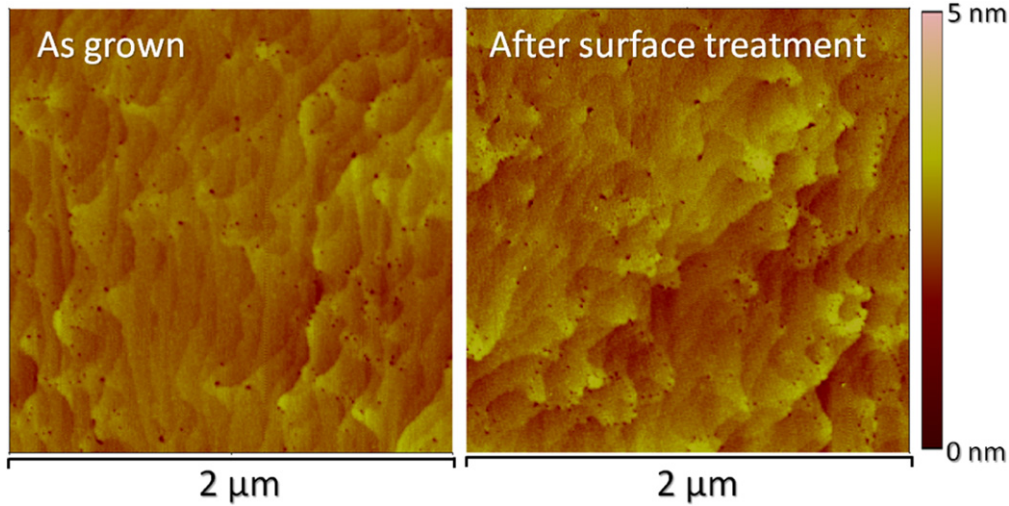
Figure 5. Comparison of the AFM images for the AlGaN/GaN HEMT sample before and after a 3-cycle surface treatment.
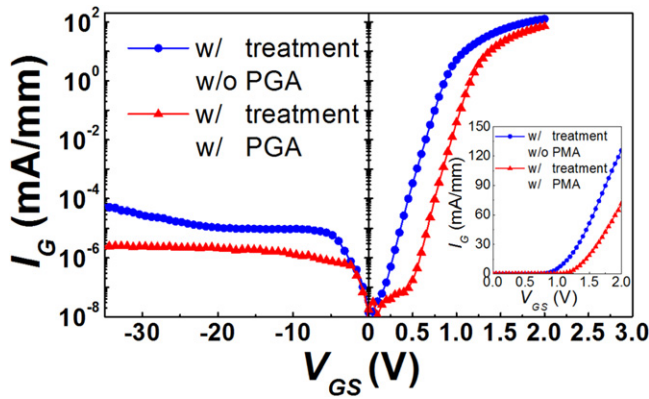

Figure 6. Reverse and forward gate leakage currents of the HEMTs with and without PGA process after elimination of the surface leakage current by surface treatment.

Figure 7. (a) Output and (b) transfer characteristics of the fabricated HEMTs with and without the two-step surface treatment and PGA process.

sate leakage current of the reference HEMT in our study was dominated by the high surface leakage current through the probing pads that was located on the exposed GaN buffer. After a 3-cycle O_2-plasma and HCl surface treatment, the pad-to-pad leakage current was reduced by over 5 orders of magnitude, which, as expected, matched with the off-state leakage current reduction in the HEMT device by surface treatment (blue curve in figure 2). It can also be seen that the influence of the second step PGA process on the lateral surface leakage current through the pads was negligible.

We believe that the surface leakage current reduction is attributed to the surface cleaning effects of the O_2-plasma and HCl treatment, i.e. partial removal of the surface trap states. To reveal the effects of the surface treatment on the chemical composition, x-ray photoelectron spectroscopy (XPS) measurements were performed for the samples with and without surface treatment. The binding energy measurement was calibrated by correcting the adventitious C $1s$ peak to 285 eV. Figure 4 compares the Ga $2p_{2/3}$ and Al $2p$ core-level spectra of both the exposed GaN buffer surface and the AlGaN barrier surface with and without surface treatment. For the exposed GaN buffer surface without surface treatment, the
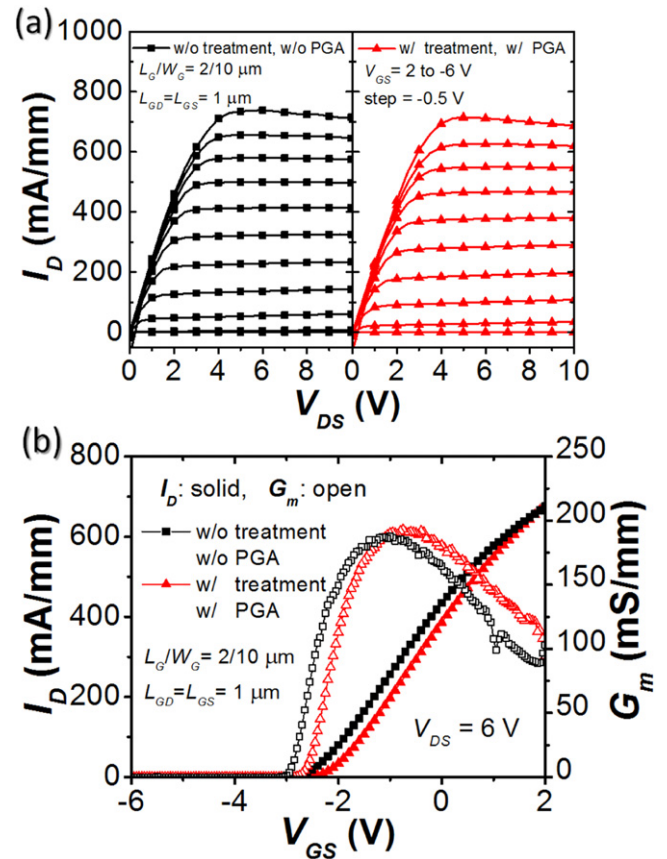
native oxide exhibits a large shoulder (Ga-O bonds accounting for 25.6%) on the higher binding energy side of the Ga-N peak. After surface treatment, the proportion of the Ga-O bonds drops to 19.8%. Removal of the native oxide is believed to greatly facilitate the surface leakage current reduction, since the poor quality native oxide (GaO_x) is one of the culprits for the high density trap states [14]. This

Table 1. Benchmark of the GaN-based HEMTs with reduced off-state leakage current by different approaches.

Structure	L_G/L_{SD} (μm)	On/off Ratio	I_{D_max} (mA/mm)	Degradation in I_{D_max}
GaN/AlGaN/GaN [6]	2/8	$\sim 10^7$	360	$\sim$10%
InAlN/GaN [8]	2/8	$\sim 10^6$	800	$\sim$20%
InAlN/GaN [11]	0.15/2	$\sim 10^{12}$	370	$\sim$40%
AlGaN/GaN [12]	2/6	$\sim 10^8$	80	$\sim$44%
p-InGaN/AlGaN/GaN [13]	2/8	$\sim 10^{10}$	126	—
GaN/ AlGaN/GaN [this work]	**2/4**	**$\sim 10^{10}$**	**750**	**<4%**
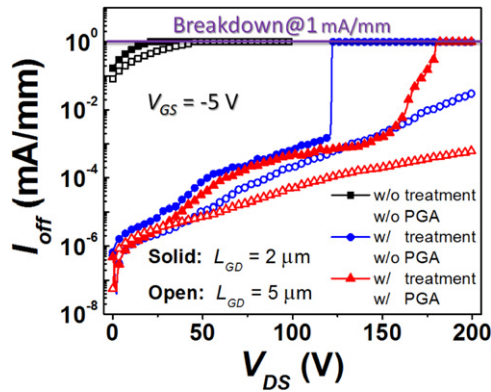
Figure 8. Three terminal off-state breakdown measurements of the HEMTs on the three samples with various L_{GD}.

mechanism is different from what was reported by Chung *et al* [9], in which a high power (800 W) O_2 plasma was used to form a layer of Ga_2O_3 gate dielectric. Different from the native oxide, the intentionally formed Ga_2O_3 had a relatively high quality and might be able to passivate the surface states. In figure 4(b) a similar decline in the concentration of Ga-O and Al-O bonds can be observed for the AlGaN barrier surface after surface treatment. It was also found that the oxygen concentration at the exposed GaN buffer surface is much higher than that of the as-grown AlGaN barrier surface, suggesting that the etched GaN surface is easier to oxidize than the as-grown epilayer surface. In addition, chlorine residues with a concentration of $\sim$2.3% has been detected on the exposed GaN buffer surface and it disappeared after the surface treatment, which might contribute to the surface leakage current reduction as well. Figure 5 compares atomic force microscopy (AFM) images of the AlGaN/GaN HEMT sample before and after a 3-cycle surface treatment. No surface degradation can be observed after the surface treatment and the root mean square (RMS) roughness across a 2 μm × 2 μm scanned area remains the same, about 0.3 nm. It indicates that the low power O_2-plasma treatment used in this work will not be able to oxidize the as-grown AlGaN barrier, which is different from what was suggested in the digital etching process [15]. All these results prove that the surface treatment process in our study is very effective in cleaning without deteriorating the sample surface.

Further reduction of the off-state leakage current by the second step PGA process is mainly attributed to the suppression of the vertical tunneling leakage path through the Schottky barrier. Figure 6 shows the reverse and forward gate

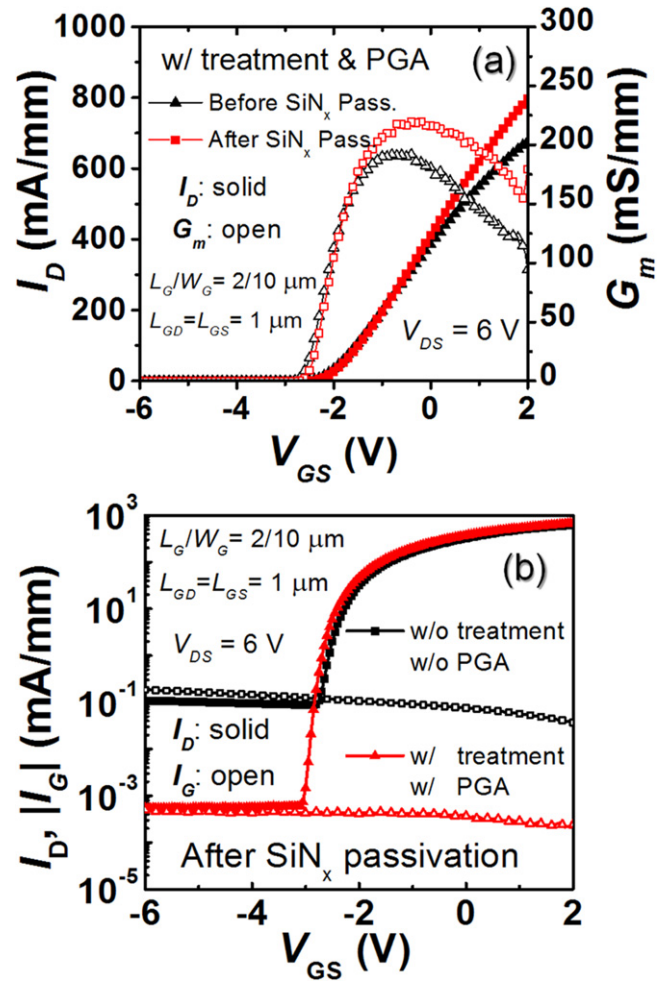**Figure 9.** (a) Comparison of the on-state performance for the fabricated HEMTs with the two-step process before and after SiN_x passivation; (b) transfer characteristics of the two passivated HEMTs with and without the two-step surface treatment and PGA process.

leakage currents of the HEMTs with and without PGA after elimination of the surface leakage current by the surface treatment. The effective barrier height ($\varnothing_b$) and the ideality factor (n) of the Schottky barrier diodes can be extracted using the standard thermionic emission mechanisms [16, 17]. The *I-V* relationship of a Schottky barrier diode is described by

$$J = J_s \left[\exp\left(\frac{qV}{nkT}\right) - 1 \right], \qquad (1)$$
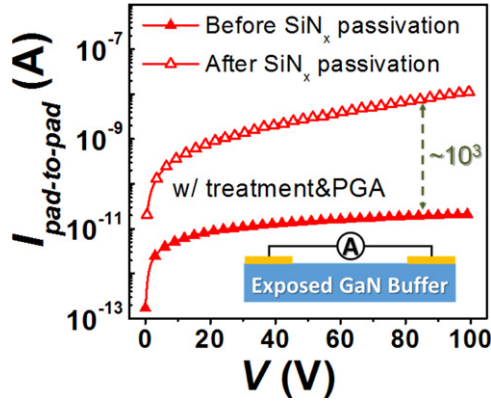
Figure 10. Comparison of leakage currents between two individual pads for the sample with the two-step process before and after SiN$_x$ passivation.

where J_s is the saturation current density

$$J_s = A^* T^2 \exp\left(\frac{-q\varnothing_b}{kT}\right),$$ (2)

q is the electron charge, V is the applied voltage, T is the absolute temperature, k is the Boltzmann constant, and A^* is the effective Richardson constant (34.2 A cm^{-2} K^{-2} for Al$_{0.25}$Ga$_{0.75}$N [16]). From the forward current characteristics in figure 6, $\varnothing_b$ of 0.82/1.03 eV and n of 1.58/1.51 were extracted for the devices without and with PGA, respectively. This result suggests an improved quality of the Shottky contact, which might be attributed to the removal of shallow traps from the Shottky contact interface by the PGA process [18]. The main reverse leakage mechanism of an AlGaN/GaN Schottky barrier diode includes both trap-assisted tunneling and direct Fowler–Nordheim tunneling [2, 11], described as

$$J_{TAT} \propto N_t E_d \exp\left[-\frac{\varnothing_t - A\sqrt{E_d}}{kT}\right]$$ (3)

and

$$J_{FNT} \propto E_d^2 \exp\left[-\frac{C\varnothing_b^{3/2}}{E_d}\right],$$ (4)

respectively. Here, $\varnothing_t$ is the trap energy below the barrier conduction band edge and $\varnothing_b$ is the barrier height. Therefore, the increased Schottky barrier height from 0.82 eV to 1.03 eV by PGA in the experiments contributes to the reduction of the reverse gate leakage current. Furthermore, a higher turn on voltage was observed for the device with PGA, as shown by the linear plot of the forward currents in the inset of figure 6. For the application of an AlGaN/GaN HEMT, high gate turn on voltage could exert favorable effects on its gate swing, power consumption and reliability.

The two-step process developed in this study introduced no obvious degradation to the device on-state drain current (I_D) and peak transconductance (G_m), as confirmed by the comparison of output and transfer characteristics between the HEMTs with and without surface treatment and PGA in figure 7. The result was benchmarked with other reported

GaN-based HEMTs in the literature using different leakage reduction approaches, as listed in table 1. Our device exhibited a comparably large on/off current ratio and maintained a relatively high on-state current. However, it should be noted that the PGA process introduced a positive shift of threshold voltage by around 0.3 V, as shown in figure 7(b).

Figure 8 compares the three terminal off-state breakdown characteristics of the HEMTs on the three samples. Significantly improved breakdown performance has been achieved by using the combined surface treatment and PGA process. The devices that went through the two-step process yielded a breakdown voltage of 180 V for $L_{GD} = 2\,\mu$m and far beyond 200 V for $L_{GD} = 5\,\mu$m. A high breakdown voltage exceeding 1500 V was measured for the device with a L_{GD} of 15 μm. In contrast, early breakdown below 50 V occurred for the control devices without surface treatment nor PGA, which was limited by their high off-state leakage current.

Dielectric passivation for a GaN-base HEMT is important to improve its stability and long-term reliability. We performed the SiN$_x$ passivation using PECVD for the two fabricated HEMTs with and without the two-step surface treatment and PGA process. Figure 9(a) compares the transfer characteristics of the device with the two-step process before and after the SiN$_x$ passivation. As expected, both on-state I_D and peak G_m were enhanced by the passivation. As shown in figure 9(b), the passivated device that went through the two-step process exhibited a much lower off-state leakage current, over two orders of magnitude, than the one without the two-step process, implying an obvious effect of the proposed two-step process (e.g., improving the resilience of the material to process-induced instabilities). However, it was found that after the passivation the off-state leakage current in the treated device increased by around three orders of magnitude. The higher off-state leakage current mainly resulted from the increased surface leakage after passivation, as confirmed by the increased pad-to-pad leakage after passivation in figure 10, and it could be due to the yet-to-optimized passivation preparation process in this study, since the passivation highly depended on not only the initial state of the surface before passivation, but also the SiN$_x$ film quality, deposition environment, etc [19]. Similarly, the surface leakage current increase after SiN$_x$ passivation has been observed by others as well [20, 21].

4. Conclusion

A two-step process involving pre-gate surface treatment and PGA has been developed to separately address the lateral surface leakage current and vertical tunneling current in AlGaN/GaN HEMTs. The lateral surface leakage current was greatly suppressed by removal of the surface trap states through a low power O$_2$-plasma and HCl surface treatment process, while the vertical gate tunneling current was lowered through improved Schottky contact quality after thermal annealing. In total, the off-state leakage current was reduced by about 7 orders after implementation of the two-step

process. As no degradation was introduced to the device on-state performance, the HEMT exhibited a high on/off current ratio of 10^{10} and steep subthreshold slope of 62 mV/dec. In addition, the two-step process has been shown to be helpful in surface preparation for device passivation by alleviating the process-induced surface instability.

Acknowledgments

References

[1] Kotani J, Tajima M, Kasai S and Hashizume T 2007 *Appl. Phys. Lett.* **91** 093501

[2] Karmalkar S, Sathaiya D M and Shur M S 2003 *Appl. Phys. Lett.* **82** 3976

[3] Chen Y, Zhang K, Cao M, Zhao S, Zhang J, Ma X and Hao Y 2014 *Appl. Phys. Lett.* **104** 153509

[4] Cao X A, Pearton S J, Dang G T, Zhang A P, Ren F and Van Hove J M 2000 *Trans. Electron Devices* **47** 1320

[5] Shul R J, Zhang L, Baca A G, Willison C G, Han J, Pearton S J, Lee K P and Ren F 2001 *Solid State Electron.* **45** 13

[6] Lee N, Lee M, Choi W, Kim D, Jeon N, Choi S and Seo K 2014 *Japan. J. Appl. Phys.* **53** 04EF10

[7] Zaidi Z H, Lee K B, Guiney I, Qian H, Jiang S, Wallis D J, Humphreys C J and Houston P A 2014 *J. Appl. Phys.* **116** 244501

[8] Ganguly S, Verma J, Hu Z, Xing H and Jena D 2014 *Appl. Phys. Express* **7** 034102

[9] Chung J W, Roberts J C, Piner E L and Palacios T 2008 *Electron Device Lett.* **29** 1196

[10] Chu R, Shen L, Fichtenbaum N, Brown D, Keller S and Mishra U K 2008 *Electron Device Lett.* **29** 297

[11] Wang R, Saunier P, Tang Y, Fang T, Gao X, Guo S, Snider G, Fay P, Jena D and Xing H 2011 *Electron Device Lett.* **32** 309

[12] Lin Y, Lain Y and Hsu S S H 2010 *Electron Device Lett.* **31** 102

[13] Deguchi T, Kikuchi T, Arai M, Yamasaki K and Egawa T 2012 *Electron Device Lett.* **33** 1249

[14] Hinkle C L, Milojevic M, Brennan B, Sonnet A M, Aguirre-Tostado F S, Hughes G J, Vogel E M and Wallace R M 2009 *Appl. Phys. Lett.* **94** 162101

[15] Wang Y, Wang M, Xie B, Wen C P, Wang J, Hao Y, Wu W, Chen K J and Shen B 2013 *Electron Device Lett.* **34** 1370

[16] Saadaoui S, Mongi Ben Salem M, Gassoumi M, Maaref H and Gaquière C 2011 *J. Appl. Phys.* **110** 013701

[17] Rao P K, Park B, Lee S, Noh Y, Kim M and Oh J 2011 *J. Appl. Phys.* **110** 013716

[18] Kim H, Lee J, Liu D and Lu W 2005 *Appl. Phys. Lett.* **86** 143505

[19] Yeluri R, Swenson B L and Mishra U K 2012 *J. Appl. Phys.* **111** 043718

[20] Liu Z H, Ng G I, Zhou H, Arulkumaran S and Maung Y K T 2011 *Appl. Phys. Lett.* **98** 113506

[21] Lin S *et al* 2015 *Electron Device Lett.* **36** 757